ANALYSIS OF COLD PATCH ON THE SEA OFF NORTHEASTERN TAIWAN

Yu-Hsin Cheng[1] and Chung-Ru Ho[2]
[1]Graduate Student, Department of Marine Environmental Informatics,
National Taiwan Ocean University, 2, Pei-Ning Rd., Keelung 20224, Taiwan;
Tel: +886-2-24622192#6345; E-mail: 29981002@mail.ntou.edu.tw

[2]Professor, Department of Marine Environmental Informatics,
National Taiwan Ocean University, 2, Pei-Ning Rd., Keelung 20224, Taiwan;
Tel: +886-2-24622192#6345; E-mail: b0211@mail.ntou.edu.tw

KEY WORDS: Cold Patch, Multi-sensor, Northeastern Taiwan, Ocean Remote Sensing

ABSTRACT: Mechanisms of the occurrence frequency of cold patch on the sea off northeastern Taiwan are analyzed using multi-sensor data from different satellites. In this study, Sea surface temperature (SST) data derived from infrared sensors, sea surface height anomaly (SSHA) data derived from satellite altimeters, as well as sea surface wind data derived from microwave scatterometers are analyzed by Empirical Orthogonal Function (EOF) and Fast Fourier Transform (FFT) methods to investigate the temporal variability of the cold patch. According to the analyses of SSHA data from 1993 to 2009 and SST data from 1985 to 2008, the variations of cold patch have an interannual oscillation around 5 years, annual cycle, and an intra-seasonal fluctuation with main peak centered at 62 days. The variations of annual and intra-seasonal periods of the cold patch may be affected by the migration of Kuroshio suggested by previous studies. Sea surface wind stress data are also analyzed. After applying a 13-month running mean filter, the primarily period of the wind stress data is an inter-annual period of around 5 years which is the same as that of SSHA and SST. It implies that generating vertical motion in the sea off northeastern Taiwan is significantly impacted by the sea surface wind filed fluctuation. This suggests that not only Kuroshio but also sea surface wind stress play roles in modifying the occurrence frequency of the cold patch on the sea off northeastern Taiwan.

1. INTRODUCTION

The sea off the northeastern coast of Taiwan is a dynamic region because the intruding Kuroshio and the northward Taiwan Warm Current converge at that place (Liang et al., 2003). The northward Kuroshio flows change direction to north-eastward when it collides with the continental shelf off northeastern Taiwan to induce upwelling over the shelf break (Chern et al., 1990; Tang et al., 1994; Sun et al., 1997). The upwelling phenomenon on the sea surface seen as a cold patch from satellite sea surface temperature images has a strong temperature drop (Figure 1). Fan (1980) analyzed hydrographic measurements and described that upwelling water has large displacements of vertical and horizontal temperature gradients. Therefore, the water mass of this phenomenon is also called cold dome.

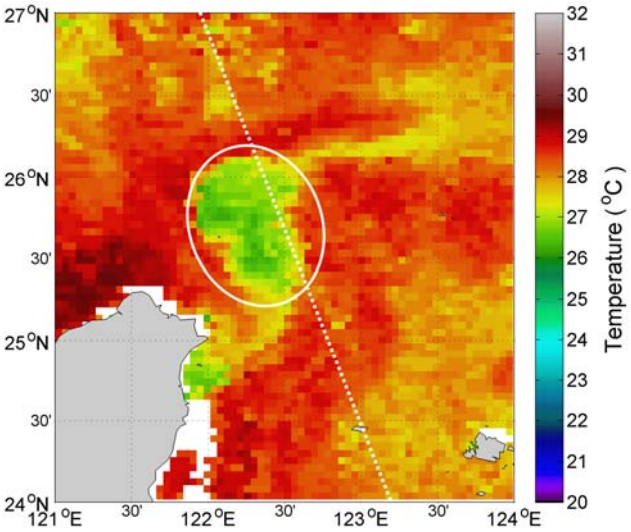

Figure 1. Advanced Very High Resolution Radiometer (AVHRR) SST image of July 29, 2006. The white circle indicates the cold patch off northeastern Taiwan. The white dotted line is the ground track (Pass 240) of T/P and Jason-1/2 satellites.

Tang et al. (1999) indicated that the vertical motion is generated because an intrusion of Kuroshio flow runs over the continental shelf region. Previous studies including satellite measurements, in-situ observations and numerical models found that the upwelling exist all year round (Lin et al., 1992; Liu et al., 1992; Wu et al., 2008). Tseng et al. (2000) collected satellite sea surface temperature (SST) images to reveal the presence of the cold patch off northeastern Taiwan in summer. Tang et al. (2000) analyzed current observations measured by shipboard Acoustic Doppler Current Profilers (ADCP) from 1995 to 1997 and indicated that the upwelling is modulated by the seasonal migration of Kuroshio. From sea surface height anomaly (SSHA) data and SST data, Cheng et al. (2009) found the intra-seasonal, annual, and inter-annual variations of the cold patch. The intra-seasonal variability may be induced by the Kuroshio migration because of its migration period of between 30 and 70 days (Hsin et al., 2008). A recent numerical study (Chang et al., 2009) showed that the seasonal variability of upwelling near the surface (about 30 m) is induced by the monsoonal change in wind stress curl.

Although previous results stated that the occurrence frequency of the upwelling is related to the Kuroshio movement and the change of wind stress curl in the intra-seasonal and annual periods, the inter-annual fluctuation about 5 years is firstly revealed (Cheng et al., 2009) and this fluctuant period could not be explained reasonably with the variability of Kuroshio mainstream. In this paper, we investigate the possible cause of the inter-annual variability of cold patch observed from SST data and SSHA data.

2. MULTI-SENSOR DATA

The data used in this study include SST, along-track SSHA data and sea surface wind stress data. They are derived from satellite infrared sensors, altimeters and scatterometers, respectively.

2.1 Sea Surface temperature

The SST data used in this study is derived from the Advanced Very High Resolution Radiometer (AVHRR) onboard the National Oceanic and Atmospheric Administration (NOAA) series satellites. The SST data are the best SST product of Pathfinder monthly average from 1985 to 2008 with 4-km spatial resolution. A spatial-temporal merged has been used to complement the lack of SST data. We define a spatial-temporal integral mean of SST as:

$$T = \frac{1}{\delta t \times S} \iiint T_i(x, y, t)\,dxdydt\,, \tag{1}$$

where T_i is the SST at position x, y and time t; and S is the integral area; and δt is the integral time.

To analyze the variation of SST, the image of monthly mean SST were generated to examine the spatial distribution and temporal variation of cold patch.

2.2 Sea surface height anomaly

The along-track SSHA data used to verify the detected cold patch is a merged product provided by the Archiving Validation and Interpretation of Satellite Data in Oceanography (AVISO). This along-track SSHA product derived from altimeters onboard the TOPEX/Poseidon (T/P) and the Jason-1/2 satellites is available at 10-day temporal interval with 6-km spatial resolution and is computed the differences between the observed sea surface height and a 7-year mean profile (1993-1999). SSHA data obtained from T/P (from January 1993 to August 2002), Jason-1 (from August 2002 to October 2008) and Jason-2 (from October 2008 to December 2008) are blended to constitute a longer-term and continuous time series data. The dotted line crossed the cold patch area (Figure 1) is the ground track of Pass 240 of T/P and Jason-1/2. Figure 2 shows the time series of SSHA of Pass 240 between 24°N and 27°N from January 1993 to December 2008. Within the dashed rectangle is the active area of upwelling.

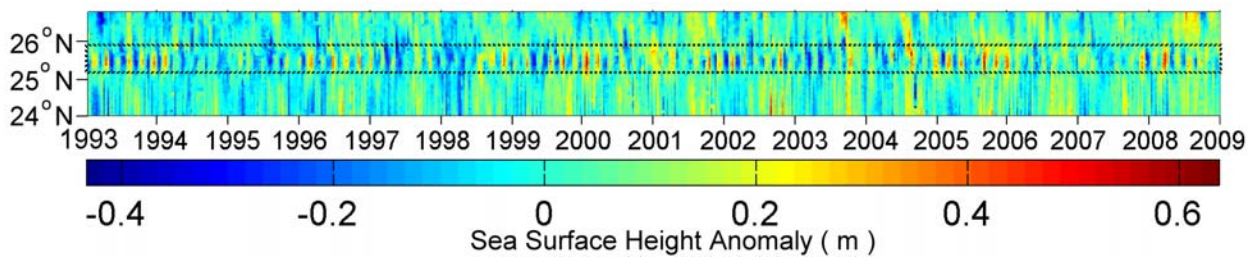

Figure 2. Time series that comprised of along-track SSHA data derived from T/P, Jason-1 and Jason-2 along Pass 240 across the upwelling area. The active area of upwelling is within the dashed rectangle off northeastern Taiwan.

2.3 Sea surface wind stress

The microwave scatterometers on the ERS-1/2 and QuikSCAT satellites measure sea surface wind velocity over the global ocean. Then, the sea surface wind stress (τ) is derived from wind velocity and is constructed by Institut français de recherche pour l'exploitation de la mer (IFREMER). The sea surface wind stress is estimated by the bulk formulation (2):

$$\tau = \left(\tau_x, \tau_y\right) = \rho C_D W\left(u, v\right) \tag{2}$$

where τ , τ_x and τ_y are the sea surface wind stress, zonal component (positive eastward) and meridional component (positive northward), respectively; ρ is the density of surface air; C_D is the drag coefficient; and W , u and v are the scatterometer wind speed, zonal component (positive eastward) and meridional component (positive northward) , respectively.

The monthly sea surface wind stress data derived from ERS-1 (from January 1992 to May 1996), ERS-2 (from June 1996 to January 2000) and QuikSCAT (from January 2001 to October 2009) satellites is used in this study. We blended these satellite data to constitute continuous time-series data and gridded them to 0.5º latitude by 0.5º longitude.

3. METHODS

In order to analyze the temporal variability of cold patch, we performed the Empirical Orthogonal Function (EOF) analysis. The EOF analysis is considered to extract some of principle components to explain most of the dominant variations of certain database and EOFs are a method usually used for partitioning the variance of a spatially distributed dataset of concurrent time series (Emery and Thomson, 2001). In this study, we focus on the inter-annual variability. Therefore, the data is applied a 13-month running mean low-pass filter to filter out the higher frequencies than annual cycle before applying EOF analysis. The sea surface wind stress data is simply partitioned off into the variance of a spatially distributed group and associated time series by EOF analysis. After applying EOF analysis, we could get several statistical modes and then analyze the time series to figure out the inter-annual phenomenon by Fast Fourier Transform (FFT).

4. EMPIRICAL ORTHOGONAL FUNCTIONS ANALYSIS

4.1 Variation of cold patch

Because the study area is often obstructed by clouds so that daily infrared SST images good enough for cold patch detection are seldom available, monthly SST data are used in this study. After applying EOF, the cold patch phenomenon is extracted efficaciously from SST data in the fourth mode of EOF (Figure 3). The first three modes of EOF analysis are the seasonal and annual fluctuations. In terms of SST, the large seasonal and annual fluctuations are dominant in northeastern Taiwan as many previous known. The result of the fourth EOF mode shows that there is a large-amplitude oscillation on the sea off northeastern Taiwan (Figure 3a). To get more understanding of the variation of the cold patch, the Fast Fourier Transform (FFT) was applied to the corresponding temporal variation. The power spectra shown in Figure 4 indicate that the main peaks are at the annual and about 5-years periods.

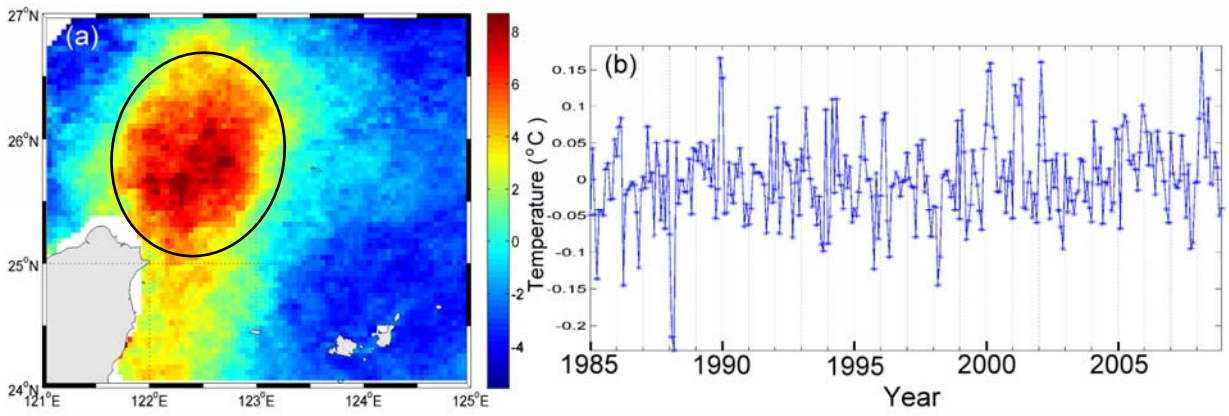

Figure 3. (a) The spatial structure of the fourth EOF mode of SST data (unit: ºC). The black circle indicates the cold patch off northeastern Taiwan. (b) The corresponding temporal variation.

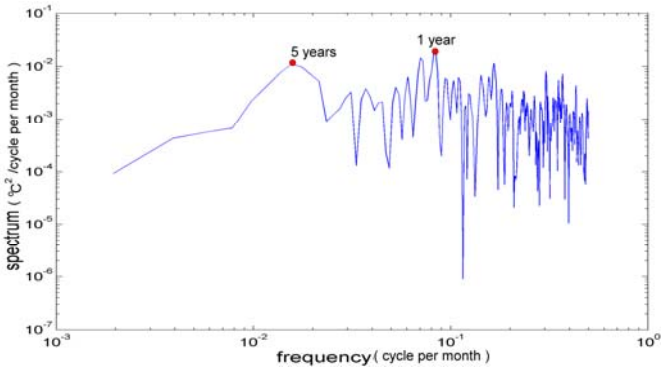

Figure 4. Power spectra of the fourth EOF temporal mode. Peaks are at the annual and 5-year periods.

Furthermore, the along-track SSHA data are used to verify the detected cold patch observed by SST. From the time series of SSHA of Pass 240 which is across the cold patch area (Figure 2), one can see that SSHA variations are more active between 25°N and 26°N (the inside of dashed rectangle) than surrounding areas. Because the mechanism of upwelling is divergence on the upper-layer ocean, the upwelling area is characterized by lower SSH relative to surrounding SSHs. The negative SSHA in blue in the active area means the possible occurrence of the cold patch. To get more understanding of the variation of the cold patch from SSHA, we also performed an EOF analysis to extract the cold patch from spatial structure and analyze the corresponding temporal variations by FFT (Figure 5).

Figure 6 shows the power spectrum density of the along-track SSHA. Three major periods including 62-days, 1-year and about 5-years can be found, which reflect the intra-seasonal, the annual and the inter-annual periods, respectively. Previous studies including satellite measurements and numerical models (Wu et al., 2008; Chang et al., 2009; Cheng et al., 2009) suggested that intra-seasonal and annual periods shown in the detecting result of cold patch are associated with seasonal migration of Kuroshio mainstream. However, the 62-day period may be not only associated with migration of Kuroshio mainstream but also aliased sea-level signals. Ray (1988) analyzed T/P sea-level spectra and found out that tidal aliases correspond to the T/P sampling rate of 9.9156 days have a 62.1-day period for M_2 tide.

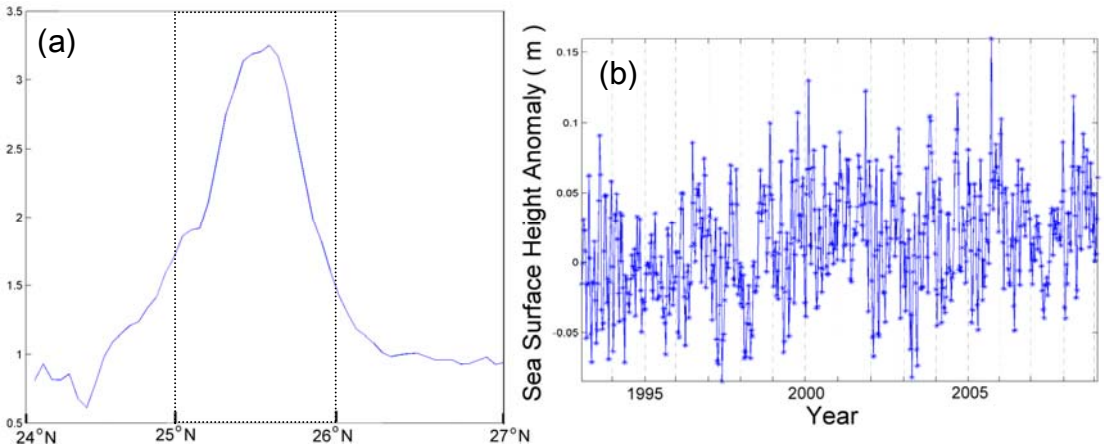

Figure 5. (a) The spatial structure of the first EOF mode for along-track SSHA data (Pass 240). The dashed rectangle indicates the cold patch off northeastern Taiwan. (b) Corresponding temporal variation.

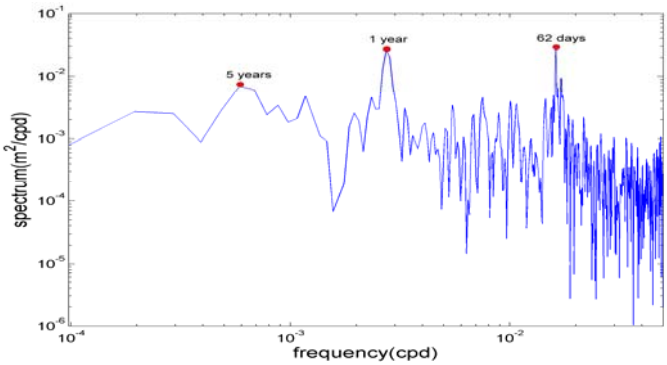

Figure 6. Power spectra for along-track SSHA across the active area off northeastern Taiwan. Peaks are at the intra-seasonal, annual and inter-annual frequencies.

In addition, the inter-annual variation (about 5 years) is firstly revealed by Cheng et al. (2009). In this study, we are more interested in inter-annual variations, and so we applied a 13-month running mean low-pass filter to filter out above two periods (annual and intra-seasonal periods) and then corresponding temporal series of SST and SSHA will be compared with sea surface wind stress in the next section.

4.2 Comparison with sea surface wind stress

The inter-annual fluctuation is often masked by the large annual fluctuation in terms of sea surface wind stress around Taiwan because Taiwan is located in the monsoon climate zone. We remove the annual cycle with a 13-month running mean low-pass filter to emphasize inter-annual variability before applying EOF analysis to the residual sea surface wind stress field off northern Taiwan. The first EOF mode accounts for 99.5% of the total variance. The temporal variation of the first mode is compared with above-mentioned SST and SSHA time series over the dynamic area (Figure 7). These four time series oscillations are almost in phase. In other words, it implies that upwelling variation may be induced by the sea surface wind stress fluctuations prompted by El Niño or La Niña. Chang et al. (2009) reported that sea surface wind stress curl could be important especially over long-terms and large scales in modulating the cold patch on the sea off northeastern Taiwan.

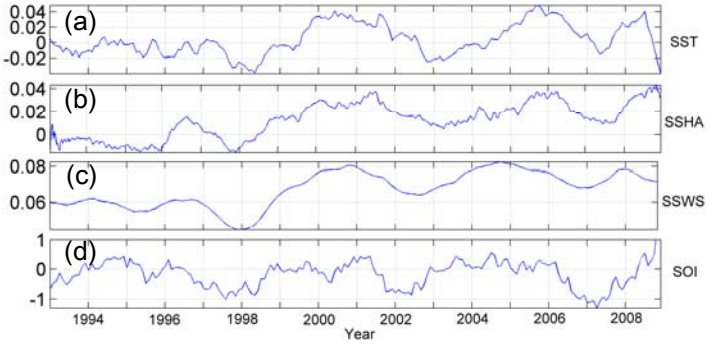

Figure 7. Comparison of AVHRR SST (a), along-track SSHA (b), sea surface wind stress (c) and southern oscillation index (d) from 1993 to 2008.

Furthermore, we applied FFT analysis, like foregoing process of SSHA time series, to find out periods of corresponding temporal variation of sea surface wind stress and southern oscillation index (SOI). In Figure 8, the main peak primarily represents an inter-annual period of around 5 years which is almost the same as that of SST and SSHA. Since the inter-annual period in SSHA and sea surface wind stress is similar which suggests that sea surface wind stress plays a role in modifying the occurrence frequency of the cold patch. However, the interaction mechanism will require to be clarified in further investigations.

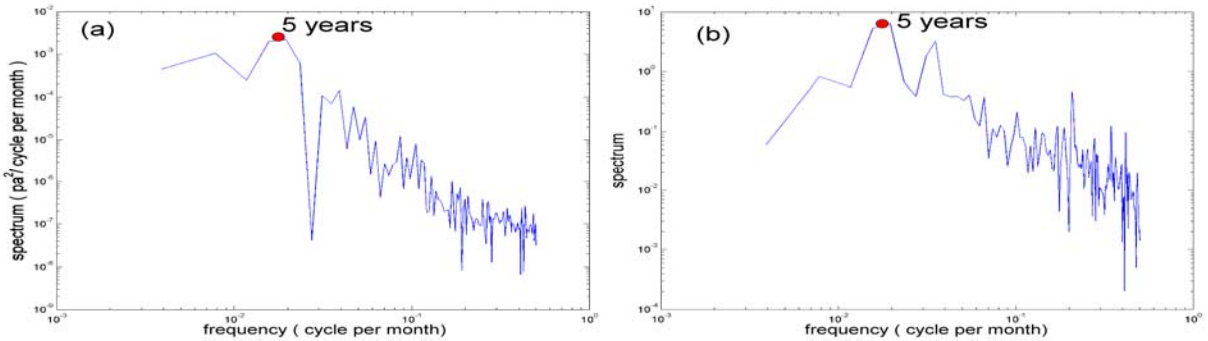

Figure 8. (a) Power spectra for corresponding temporal variation of sea surface wind stress. (b) Power spectra of SOI. Peaks of both power spectra are around 5-years period.

5. CONCLUSIONS

The SST data derived from infrared sensors and along-track SSHA data derived from altimeters across the upwelling area over the shelf off the northeastern coast of Taiwan have been used to investigate the temporal variability of the cold patch. After applying EOF, the cold patch is extracted efficaciously in the fourth and the first mode of EOF from SST and SSHA data, respectively. The corresponding temporal distribution of SST and SSHA reveals the intra-seasonal, the annual and the inter-annual periods. This large-scale variability is confirmed by the FFT analysis on SST and along-track SSHA data extracted from the cold patch region. The main peak of spectrum is about 5 years.

Sea surface wind stress data and SOI are also analyzed. There are similar inter-annual oscillations in SST, SSHA, sea surface wind stress data off northeastern Taiwan and SOI. In other words, the oscillation of these time series are in phase. Sea surface wind stress fluctuations were prompted by El Niño or La Niña. Wind forcing was responsible for sea surface motion in this upwelling region (Chang et al., 2009). The temporal variation of sea surface wind stress and SOI also reveals a nearly 5-year period. This result implies that sea surface wind stress is the long-term and large-scale processes playing a role in modifying the occurrence frequency of cold patch. In addition, it suggests that wind stress also plays an important role expect for the Kuroshio in this upwelling region near the shelf break off the northeastern coast of Taiwan.

REFERENCES

Liang, W.-D., T.-Y. Tang, Y.-J. Yang, M.-T. Ko, and W. S. Chuang, 2003. Upper-ocean currents around Taiwan. Deep-Sea Res. Pt. II., 50, pp. 1085-1105.

Chern, C.-S., and J. Wang, 1990. On the Kuroshio branch current north of Taiwan. Acta Oceanogr. Taiwan , 25, pp. 55-64.

Tang, T.-Y., and T.-T. Wen, 1994. Current on the edge of the continental shelf northeast of Taiwan. Terr. Atmos. Oceanic Sci., 5, pp. 335-348.

Sun, X.P., and S.M. Xiu, 1997. Analysis on the cold eddies in the sea area northeast of Taiwan. Mar. Sci. Bull., 16, pp. 1-10.

Fan, K.-L., 1980. On the upwelling off northeastern shore of Taiwan. Acta Oceanogr. Taiwan, 11, pp. 105-117.

Tang, T.-Y., Y. Hsueh, Y.-J. Yang, and J. C. Ma, 1999. Continental slope flow northeast of Taiwan. J. Phys.Oceanogr., 29, pp. 1353-1362.

Lin, C.Y., C.Z. Shyu, and W.H. Shih, 1992. The Kuroshio fronts and cold eddies off northeastern Taiwan observed by NOAA-AVHRR imageries. Terr. Atmos. Oceanic Sci., 3, pp. 225-242.

Liu, K.K., G.C. Gong, S.W. Lin, C.Y. Yang, C.L. Wei, S.C. Pai, and C.K. Wu, 1992. The year-round upwelling at the shelf break near the northern tip of Taiwan as evidenced by chemical hydrography. Terr. Atmos. Oceanic Sci., 3, pp. 243-276.

Ray, R.-D., 1998. Spectral analysis of highly aliased sea-level signals. J. Geophys. Res., 103, pp. 24991-25003.

Wu, C.-R., H.-F. Lu, and S.-Y. Chao, 2008. A numerical study on the formation of upwelling off northeast Taiwan. J. Geophys. Res., 113, C08025, doi:10.1029/2007J C004697.

Tseng, C., C. Lin, S. Chen, and C. Shyu, 2000. Temporal and spatial variations of sea surface temperature in the East China Sea, Cont. Shelf Res., 20, pp. 373-387.

Tang, T.-Y. J.-H. Tai, and Y.-J. Yang, 2000. The flow pattern north of Taiwan and the migration of the Kuroshio. Cont. Shelf Res., 20, pp. 349-371.

Cheng, Y.-H., C.-R. Ho, Z.-W. Zheng, Y.-H. Lee, and N.-J. Kuo, 2009. An algorithm for cold patch detection in the sea off Northeast Taiwan Using multi-sensor data, Sensors, 9, pp. 5521-5533.

Chang, Y.-L., C.-R. Wu, and L.-Y. Oey, 2009. Bimodal behavior of the seasonal upwelling off the northeastern coast of Taiwan. J. Geophys. Res., 114, C03027, doi:10.1029/2008JC005131.

Hsin, Y.-C., C.-R. Wu, and P.-T. Shaw, 2008. Spatial and temporal variations of the Kuroshio east of Taiwan, 1982-2005: A numerical study. J. Geophys. Res., 113, C04002, doi:10.1029/2007JC004485.

Emery, W. J., and R. E. Thomson, 2001, Data Analysis Methods in Physical Oceanography, Elsevier, New York, pp. 319-325.

ACKNOWLEDGMENTS

This work is supported by the National Science Council of Taiwan through grant NSC 98-2611-M-019-017-MY3. The authors would like to thank PO.DACC/NASA, AVISO/CNES, and IFREMER for providing the AVHRR image, sea surface height data, and sea wind data, respectively.